BINDING SITE FLEXIBILITY: MOLECULAR SIMULATION OF PARTIAL AND FULL AGONISTS WITHIN A GLUTAMATE RECEPTOR.

Yalini Arinaminpathy, Mark S.P. Sansom and Philip C. Biggin*

Structural Bioinformatics and Computational Biochemistry,
Department of Biochemistry,
The University of Oxford,
South Parks Road,
Oxford,
OX1 3QU,
U.K.

FLEXIBILITY OF THE GLUTAMATE RECEPTOR BINDING POCKET

Corresponding Author:

Dr Philip Biggin
Structural Bioinformatics and Computational Biochemistry,
Department of Biochemistry,
The University of Oxford,
South Parks Road,
Oxford,
OX1 3QU,
U.K.

E_mail: phil@biop.ox.ac.uk

Telephone: +44 1865 275255

Fax: +44 1865 275273

Text pages = 16
Number of Tables = 2
Number of Figure = 5
Number of references = 47
Words in abstract = 236
Words in Introduction = 747
Words in Results and Discussion = 2472

iGluR; ionotropic Glutamate Receptor.
AMPA; α-amino-3-hydroxy-5-methyl-4-isoxazole propionic acid.
NMDA; N-methyl-D-aspartate.
LBD; Ligand Binding Domain.
RMSD; Root Mean Square Deviation.
RMSF; Root Mean Square Fluctuation.

Abstract

Ionotropic glutamate receptors mediate fast synaptic transmission in the mammalian central nervous system and play an important role in many different functions including memory and learning. They have also been implicated in a variety of neuropathologies and as such have generated widespread interest in their structure and function. Molecular Dynamics simulations (5 x 20 ns) of the ligand-binding core of the GluR2 glutamate receptor have been performed. Through simulations of both wild-type and the L650T mutant, we show that the degree of protein flexibility can be correlated with the extent to which the binding cleft is open. In agreement with recent experiments, the simulations of kainate with the wildtype construct show a slight increase in β-sheet content which we are able to localize to two specific regions. During one simulation, the protein made a transition from an open-cleft conformation to a closed-cleft conformation. This closed cleft conformation closely resembles the closed-cleft crystal structure thus indicating a potential pathway for conformational change associated with receptor activation. Analysis of the binding pocket suggests that partial agonists possess a greater degree of flexibility within the pocket which may help to explain why they are less efficient at opening the channel than full agonists. Examination of water molecules surrounding the ligands reveals that mobility in distinct sub-sites can be a discriminator between full and partial agonism and will be an important consideration in the design of drugs against these receptors.

Introduction

The ionotropic glutamate receptors (iGluR) receptors are a family of ligand-gated ion-channels that open in response to the binding of glutamate and are responsible for fast excitatory neurotransmission in vertebrate central nervous systems. In humans, dysfunction of iGluRs has been implicated in a wide variety of neuropathologies (Dingledine et al., 1999). IGluRs have been classified according to their sequences and the pharmacology of their responses to a variety of ligands (Holman and Heinemann, 1994). Those receptors (GluR1-4) that show greatest sensitivity to the agonist α-amino-3-hydroxy-5-methyl-4-isoxazole propionic acid (AMPA) are termed AMPA receptors (Borges and Dingledine, 1998). Likewise, those that show greatest sensitivity to kainate (GluR5-7, KA1-2) and referred to as kainate receptors (Chittajallu et al., 1999; Lerma et al., 1997). Receptors that are activated by N-methyl-D-aspartate (NMDAR1, NMDAR2a-d) are called NMDA receptors (Yamakura and Shimoji, 1999). *In vivo*, NMDA receptors require both glutamate and glycine to bind for activation.

The overall architecture of iGluR (Figure 1) consists of two extracellular domains and a transmembrane (TM) domain. The ligand-binding domain, the crystal structure of which is known (Armstrong et al., 1998), forms the second extracellular domain. It is made up of two polypeptide segments (called S1 and S2) which discontinuously form the two sub-domains (or lobes) referred to as D1 and D2 (Figure 1). The transmembrane domain is inserted in between the S1 and S2 segments. Thus, the polypeptide chains exits from the D2 sub-domain as the S1 segment to form the two transmembrane helices (M1 and M2) plus a P-loop (a transmembrane architecture reminiscent of that of the potassium channel KcsA (Kuner et al., 2003; Pang et al., 2003)) then forming the S2 peptide segment which re-enters the D2 sub-domain. The chain then crosses the membrane to form a third TM helix, M3, followed by a short intracellular C-terminal

region. In addition to the similarity in the transmembrane domain to potassium channels, functional evidence (Mano and Teichberg, 1998; Rosenmund et al., 1998) and electron microscopic images (Safferling et al., 2001) indicate that glutamate receptors are tetrameric assemblies.

In each of the subunits, the ligand binding site is situated in the cleft between the D1 and D2 sub-domains with differences in the binding pocket reflecting the different agonist specificity (Armstrong and Gouaux, 2000). The proposed mode of action for this receptor family is indeed one in which the two halves of the ligand-binding domain behave as two fairly rigid sub-domains that open and close in a "clam-shell" fashion. (Mano et al., 1996). The natural agonist glutamate helps to stabilize the closed-cleft conformation of the ligand binding domain thus favouring the open-state of the channel.

Kainate (Figure 1C) is a partial agonist in that it elicits currents (from homomeric GluR4 receptors) that are ~8 fold smaller than those elicited by AMPA or glutamate (Swanson et al., 1997). The kainate-bound crystal structure showed an intermediate degree of domain closure compared to the open-apo-state and glutamate-bound structures. This partial closure of the ligand-binding domain appears to be due to steric hindrance from the isoprenyl group of the kainate molecule (Figure 1B). As a consequence, two key residues which line the binding pocket, L650 and Tyr450, are held further apart that in structures with full agonists bound. This has been addressed by mutagenesis and subsequent crystallography studies where it was shown an L650T mutation could induce a larger degree of domain closure consistent with that of a full agonist (Armstrong et al., 2003b).

It has been proposed that the degree of cleft separation is a determinant of the efficacy of the agonist (Armstrong and Gouaux, 2000). This proposal is however complicated by the fact

that partial agonists have also been shown to give single conductances similar to full agonist but with a reduced open-probability (Jin et al., 2003). We were thus interested to see to what extent flexibility and dynamics might play with respect to the behaviour of the ligand-binding cleft. We report here multiple long simulations (20ns) of both full and partial agonist bound systems. We find that the kainate-bound simulation displays much higher protein fluctuation as indicated by somewhat shorter simulations performed previously (Arinaminpathy et al., 2002). We also observe ligand flexibility such that interactions within the binding site can be mediated by water molecules. We are also able to report on the stability of waters within sub-sites around the ligand (Figure 1D), which may have important consequences for drug-design. Finally we examine the effect of the L650T mutation and compare the changes in dynamics with respect to the wildtype receptor.

Materials and Methods

The simulations described use a similar protocol to that described by us in previous simulations (Arinaminpathy et al., 2002). Briefly, crystal structures (Armstrong and Gouaux, 2000) for the glutamate (1FTJ), kainate-bound (1P1N, 1FW0) and the apo states (1FT0) of the S1S2 construct were downloaded from www.rcsb.org (Berman et al., 2000). Sequence positions are numbered according to the predicted mature polypeptide. Missing atoms were added in Quanta (Accelrys, San Diego, CA) and the N and C termini were acetylated and amidated respectively to mimic the continuation of the protein chain. Residues were modeled in their default ionization states as pKa calculations (Adcock et al., 1998) did not reveal any unusual protonation states for a system at pH=7. Crystallographic water molecules within 4Å of the protein were retained and each system was placed in a box of water of about 11000 simple point charge (SPC) waters (Hermans et al., 1984) and the appropriate number of counter ions needed to ensure neutrality. Counter ions were positioned such that they were in bulk solvent. From previous comparative studies (Pang et al., 2005) where several similar proteins from this fold-family were simulated and compared, we are confident that positioning in this way is not critical to the overall dynamics of the protein. All systems were energy minimized and subjected to a short (200ps) restrained molecular dynamics run whereby the protein (and ligand if present) heavy atoms were restrained by an harmonic force of 1000 kJ mol^{-1}nm^{-2}. After this period, all restraints were removed, except for bond-lengths which were restrained with the LINCS (Hess et al., 1997) algorithm, and the simulations ran for 20ns. For analysis that was dependent on an average property such as RMSF, the first two nanoseconds were discarded and treated as equilibration based on analysis of RMSD plots of individual sub-domains. Electrostatics were evaluated with Particle Mesh Ewald (Darden et al., 1993; Essman et al., 1995) and a 10Å cut-off.

The temperature was coupled with the Berendsen thermostat (Berendsen et al., 1984) at 310K

and a τ_T of 0.1ps. The integration time step was 2 fs and coordinates were saved every 5ps. All

simulations were performed with GROMACS (http://www.gromacs.org, (Berendsen et al., 1995;

Lindahl et al., 2001)) with the Gromacs forcefield. Cluster analysis was performed using the

linkage algorithm within the GROMACS codes.   Molecular figures were generated with

Molscript (Kraulis, 1991) and rendered with Raster3D (Merritt and Bacon, 1997).

Results and Discussion

Simulation Stability and Conformational Drift

A first pass measure of the stability and conformational drift of a protein in a simulation is

provided by the root mean squared deviation (RMSD) of the protein coordinates from their initial

values as a function of time (Figure 2A).   It can be seen that the RMSD of protein in the

presence of glutamate tends to a plateau within 3-4 ns with small fluctuations around a value of

~2 Å. In contrast, the protein with kainate present exhibits a much larger degree of fluctuation

around a slightly higher value (2.3 Å).   This is in agreement earlier shorter simulations

(Arinaminpathy et al., 2002). By plotting the RMSD of the Cα atoms of secondary structure

elements of individual sub-domains (ie. D1 with respect D1), we found that this increased

fluctuation was attributable to the D1 domain (Figure 2B and 2C). The fluctuation for the partial

agonist kainate in the D2 domain is indistinguishable from the fluctuations observed for the full

agonist, glutamate. This supports the hypothesis that the D2 lobe may simply act as a rigid

domain to pull the channel region open (Armstrong et al., 2003b).   The root mean square

fluctuation (RMSF) provides another way in which to examine protein flexibility (Figure 2D).

The general trend is well preserved across the simulations, with the largest fluctuations occurring

at loop regions. Of the two strands that connect the D1 and D2 sub-domains (residues 493 to 500

and residues 727 to 734) the second strand exhibits larger fluctuations in the Open-Apo

simulation consistent with NMR experiments where these regions are shown to be in one of the

more mobile regions of the GluR2 construct (McFeeters and Oswald, 2002).

Domain closure and inter-sub-domain motions

Comparison of the crystal structures of the LBD constructs with and without agonists

suggested that the degree of domain closure between the two sub-domains could be responsible

for differences in the effectiveness of the ligands as agonists. In addition, it was hypothesised

(Armstrong et al., 2003a) that the effectiveness of kainate could be increased by mutation of the

'doorkeeper' residue Leu650 to a smaller residue to enable greater domain closure. These aspects

were explored further in these simulations in terms of inter-sub-domain motions, i.e. how the

motion of the domains is influenced by the presence and type of ligand. In this analysis, the

inter-sub-domain separation is defined as the distance between the centres of mass of the two

sub-domains (Figure 3). At the beginning of the simulation, the proteins can be ordered in terms

of decreasing inter-sub-domain distance as Open-Apo > WT-Kai ~ L650T-Kai > Closed-Apo ~

Glu, as expected.

The separation in the Closed-Apo and Glu simulations remains reasonably constant at ~

24 Å with more fluctuation apparent in the Closed-Apo simulation confirming that these undergo

the least amount of conformational fluctuations (as observed in the RMSD analysis) and remain

'closed' over the duration of the simulations. At 0 ns, both the L650T-Kai and WT-Kai

simulations exhibit comparable inter-sub-domain separations of ~25.3 Å and ~25.0 Å

respectively. Over 20 ns, a small increase in the separation between the sub-domains is seen in

the WT-Kai simulation resulting in a separation of ~ 25.9 Å at 20 ns. Although larger fluctuations

are exhibited in the L650T-Kai simulation over the duration of the simulation, the mean

(averaged over the last 10 ns of the simulation) separation of ~25.1 Å ± 2.7 Å is significantly

smaller than that between the sub-domains in the WT-Kai system. In comparison, for the Glu

simulation, the separation remains constant at ~24 Å. Interestingly, there is ~1 Å difference in

inter-sub-domain separations in the order Glu < WT-Kai< L650T-Kai.

The Open-Apo simulation undergoes the most change in inter-sub-domain separation

(Figure 3A). In the first ~5 ns, the protein undergoes substantial fluctuations and the separation

drops by ~2 Å to adopt a separation close to that of the glutamate-bound structure, i.e. the Open-

Apo structure had switched to a 'closed' conformation. From this analysis and from visual

inspection of the Open-Apo trajectory, it appears that the two sub-domains move together to

generate a structure resembling the closed form of the ligand-binding domain similar to the Glu

bound structure. The "most closed" form of the Open-Apo simulation was found to be at ~16 ns.

The Cα RMSD at 15.96 ns between the Open-Apo and glutamate-bound crystal structure was 1.8

Å (Figure 3B) which indicates that the simulation is able to move between the two observed

states of the protein. An overlay of the two conformations is shown in Figure 3C. The change in

the radius of gyration between these two extremes is 0.8Å which is consistent with the difference

between the radius of gyration reported for the Open-Apo and Glu-bound crystal structures

(Armstrong and Gouaux, 2000). We also used the program hingefind (Wriggers and Schulten,

1997) to compare the degree of sub-domain closure using only secondary structural elements (to

remove the influence of loop motions). The difference in the extent of domain-closure between

the Open-Apo crystal configuration and the snapshot at 15.96 ns was 9° which is very similar to

the extent of domain-closure between the Open-Apo and glutamate-bound crystal structures (7°).

Thus we are confident that we are moving between the two crystallographically observed extremes.

Essential dynamics analysis was carried out on the trajectories of all the simulations. From the total fluctuations of a molecule, it is possible to extract the dominant dynamical modes responsible for the principal conformational transitions. Analysis of the Open-Apo simulation revealed that 81% of the motion was encompassed by the first 10 eigenvectors. For the Closed-Apo, WT-Kai, L650T-Kai and Glu simulations, 73%, 64%, 65% and 58% respectively of the total motion was encompassed by the first 10 eigenvectors. The first two eigenvectors of the Open-Apo simulation corresponded to very distinct motions. Eigenvector1 was a hinge-bending motion between the D1 and D2 sub-domains and eigenvector 2 a twisting motion of D1 relative to D2. Thus, the simulation has provided details of a *pathway* for sub-domain closure within the GluR2 ligand-binding domain. Although this motion occurs on a relatively fast timescale (of the order of nanoseconds) our observations of similar motions across a range of proteins possessing this fold (Pang et al., 2003; Pang et al., 2005) gives us confidence that this motion is functionally relevant.

Secondary structure changes upon ligand-binding

We examined the secondary structure content throughout the simulation, which in general was very well preserved. However, we did observe a subtle and interesting difference between the WT-Kai and the L650T-Kai simulations. We found that kainate binding in the wild-type complex (WT-Kai) promotes the formation of β-sheet structure. This finding is supported by Fourier transform infrared spectroscopic studies on the ligand-binding domain of GluR4 (Jayaraman et al., 2000), where an increase in the β-sheet content of the protein was observed as

a result of kainate binding to the wild-type receptor. In our simulations this increase in β-sheet

content can be localized to two regions in the D1 sub-domain (see Figure 4A and 4C). The first

region corresponds to residues 453-460 (region I in Figure 4A and 4C) and the second region

corresponds to loop 2 of this receptor (region ii in Figure 4A and 4C). We note here that the

regions that tend to β-sheet formation encompass residues Thr480 and Pro478 (Figure 4C) which

form part of the binding pocket. Interestingly, no such sheet formation was observed for the

L650T-WT simulation (Figure 4B).

Behaviour of the Binding Pocket.

In all simulations the ligand displayed little movement with respect to the binding pocket.

For the glutamate and L650T-Kai simulations, the distributions for all three dihedrals (C-C_α-C_β-

C_γ, C_α-C_β-C_γ-C_δ and N-C_α-C-O) examined were unimodal indicating one stable bound

conformation over the duration of the 25 ns simulation. In contrast, WT-Kai exhibited carboxyl

group flipping with respect to the dihedral N-C_α-C-O, indicating a little more flexibility whilst

not changing the binding mode *per se*. Cluster analysis (cut–off = 0.4 Å) revealed only a single

cluster found for bound ligand in the Glu simulation, whilst kainate in the WT-Kai simulation

gave 8 clusters and only 3 in the L650T-Kai simulation. These results support the suggestions

that the partial agonist kainate in the WT complex is less rigidly bound than glutamate and also

that kainate in the L650T mutant will behave with intermediate properties.

Given the difference in the apparent flexibility of the protein we wanted to investigate the

behaviour of the ligands in the binding pocket. Glutamate exhibits very little change in its

orientation and conformation within the binding pocket. Kainate appears to posses slightly more

freedom, perhaps due to the more open nature of the cleft, but all the key interactions reported in

the crystal structure complex are maintained throughout the simulation. As the positions of water

molecules within this binding pocket are thought to play a central role in agonist binding we

investigated their behaviour.   In particular we were interested in the mobility of the water within

and around the sub-sites surrounding the ligand (as described by (Armstrong and Gouaux,

2000)).   Through the course of the simulations we noted that water molecules were able to

penetrate into the binding pocket and interact with the ligand and protein within and around these

sub-sites (Figure 5). In order to broadly quantify the mobility between each simulation, we

simply summed the number of different waters making similar contacts (between ligand and

protein) within each of the sub-site regions. The results (Table 2) are very clear cut and are able

to discriminate between a full agonist (glutamate) and a partial agonist (kainate) purely on the

rate of water exchange within the binding pocket.   Furthermore, an intermediate level of

exchange is observed for the L650T mutant which behaves more like a full agonist than a partial

agonist (Armstrong et al., 2003b). In the case of the Glu and L650T-Kai simulations, sub-site E

had at least one water that persisted for more than 50% of the time. This site in the WT-Kai

simulation was a site of frequent exchange as was the case for sub-site D. The increased amount

of flexibility within the binding pocket and increased cleft opening in the WT-KAI simulation

also manifests itself at the A and B sub-sites, where solvent is able to frequently penetrate and

interrupt the direct protein-ligand interactions made by Arg485 and Pro478 (Figure 5B). This

suggests that there is room for expansion within the binding pocket such that larger ligands might

be able to at least fit into the binding pocket. We would anticipate that such ligands would be

even weaker agonists that kainate. The behaviour of water surrounding sub-site D principally

reflects a key water identified in a series of crystallographic studies (Armstrong and Gouaux,

2000) and more recently has been suggested to play a central role in GluR1/GluR2 versus

GluR3/GluR4 selectivity (Frandsen et al., 2005; Hogner et al., 2002).

A further interesting conformational change is observed at 8.78 ns where the conformation of the protein and the position of the kainate change slightly such that a water bridging the NH group of Glu705 with the Kai-γ-CO_2 group is forced out of the binding pocket and the Glu705-NH makes a direct interaction with the ligand instead (Figure 5B).

The glutamate ligand within the protein is extremely stable, and although the waters freely swap interaction sites within the binding pocket, the fact that crystallographically positioned waters are still within the binding pocket reflects the closed-cleft nature of this form of the protein. Despite this stability, there is some flexibility with the pocket. We observed that Arg485 could occasionally flip out for periods of time ranging from tens of picoseconds through to over one nanosecond. During the flip, water molecules were able to penetrate and bind with the α-carboxy moiety of the glutamate. Arg485 would then swing back in pushing the water out such that the originally observed direct interaction was regained (See Supplementary Figure 1 for snapshots of this process).

We also examined the behaviour of the Thr650 in the Kai-L650T mutation. We found that the threonine could flip (around its Cα-Cβ bond) such that it would push a water (in a position corresponding to W2 in the crystal structures) out and form a direct interaction with the Kai-γ-CO_2 group (see Supplementary Figure 2 for snapshots). When the threonine returns to its starting conformation, water is again able to return to that region to make an interaction with the Kai-γ-CO_2 group again.

We also examined the behaviour of the waters within the binding pocket of the apo simulations. Water moved relatively freely within the pocket indicating that the presence of ligands is necessary to localize water to specific sites.

Critical evaluation of methodology.

It should be remembered here that this study as with other recent studies (Arinaminpathy et al., 2002; Armstrong and Gouaux, 2000; McFeeters and Oswald, 2002) is based upon the artificial construct that corresponds to the ligand-binding domain of the full-length protein. However, given that the ligand-binding affinities for the construct mirror those observed in the full-length receptor (Chen et al., 1995; Kuusinen et al., 1995) we have some confidence that ligand-protein interactions in the single domain construct accurately reflect those in the intact receptor. Further support for this is provided by visible absorption spectroscopy studies (Deming et al., 2003) that demonstrate the same electronic environment for the antagonist CNQX in the isolated ligand-binding domain as in homomeric GluR4 receptors transiently expressed in HEK-293 cells. We should also recall that the current simulation studies are on the monomeric ligand-binding domain. It should be pointed out here that the current simulations are short relative to the timescale of physiological activation of GluR channel (recent laser-pulse photolysis experiments with caged glutamate suggest the fastest opening time for GluR2 channels to be 17 μs (Li et al., 2003) and for GluR1 channels ~35 μs (Li and Niu, 2004) and similar microsecond timescales for opening were reported for experiments performed on rat hippocampal neurons where a mixture of non-NMDA subunits are expressed (Li et al., 2002)).

Conclusions

We have shown here how the flexibility of the protein appears to depend on the agonist present and also the degree of domain-closure. That the structures maybe more flexible than perhaps first suggested has been recently supported by the observation that AMPA appears to adopt multiple-binding modes to the L650T mutation (Armstrong et al., 2003b). We have also

shown how the protein may move between an open and a closed state. Furthermore, we have

shown how water mobility within the binding pocket can be correlated with degree of domain

closure and the agonist present. Knowledge of the behaviour of these waters should help to

improve the rational design of drugs against these proteins. This will be even more important in

the kainate-selective receptors where the cavity is larger (Mayer, 2005; Nanao et al., 2005; Naur

et al., 2005) and thus consideration of the water behaviour will be critical.

References

Adcock C, Smith GR and Sansom MSP (1998) Electrostatics and the selectivity of ligand-gated ion channels. *Biophys. J.* **75**:1211-1222.

Arinaminpathy Y, Sansom MSP and Biggin PC (2002) Molecular dynamics simulations of the ligand-binding domain of the ionotropic glutamate receptor GluR2. *Biophys. J.* **82**:676-683.

Armstrong N and Gouaux E (2000) Mechanisms for activation and antagonism of an AMPA-sensitive glutamate receptor: Crystal structures of the GluR2 ligand binding core. *Neuron* **28**:165-181.

Armstrong N, Mayer ML and Gouaux E (2003a) Tuning activation of the AMPA-sensitive GluR2 ion channel by genetic adjustment of agonist-induced conformational changes. *Proc. Nat. Acad. Sci. USA* **100**:5736-5741.

Armstrong N, Mayer ML and Gouaux E (2003b) Tuning activation of the AMPA-sensitive GluR2 ion channel by genetic adjustment of agonist-induced conformational changes. *Proc Natl Acad Sci USA* **100**:5736-5741.

Armstrong N, Sun Y, Chen G-Q and Gouaux E (1998) Structure of a glutamate-receptor ligand-binding core in complex with kainate. *Nature* **395**:913 - 917.

Berendsen HJC, Postma JPM, van Gunsteren WF, DiNola A and Haak JR (1984) Molecular dynamics with coupling to an external bath. *J. Chem. Phys.* **81**:3684-3690.

Berendsen HJC, van der Spoel D and van Drunen R (1995) GROMACS: A message-passing parallel molecular dynamics implementation. *Comp. Phys. Comm.* **95**:43-56.

Berman HM, Westbrook J, Feng Z, Gilliland G, Bhat TN, Weissig H, Shindyalov IN and Bourne PE (2000) The Protein Data Bank. *Nucleic Acids Res.* **28**:235-242.

Borges K and Dingledine R (1998) AMPA receptors: molecular and functional diversity. *Prog. Brain Res.* **116**:153-170.

Chen C-C, Akopian AN, L. S, Colquhuon D, Burnstock G and Wood JN (1995) A P2X purinoceptor expressed by a subset of sensory neurons. *Nature* **377**:428-431.

Chittajallu R, Braithwaite SP, Clarke VR and Henley JM (1999) Kainate receptors: subunits, synaptic localization and function. *Trends Pharmacol. Sci.* **20**:26-35.

Darden T, York D and Pedersen L (1993) Particle mesh Ewald - an N.log(N) method for Ewald sums in large systems. *J. Chem. Phys.* **98**:10089-10092.

Deming D, Cheng Q and Jayaraman V (2003) Is the isolated ligand binding domain a good model of the domain in the native receptor? *JBC* **278**:17589-17592.

Dingledine R, Borges K, Bowie D and Traynelis SF (1999) The glutamate receptor ion channels. *Pharmacol. Rev.* **51**:7-61.

Essman U, Perera L, Berkowitz ML, Darden T, Lee H and Pedersen LG (1995) A smooth particle mesh Ewald method. *J. Chem. Phys.* **103**:8577-8593.

Frandsen A, Pickering DS, Vestergaard B, Kasper C, Nielsen BB, Greenwood JR, Campiani G, Fattorusso C, Gajhede M, Schousboe A and Kastrup JS (2005) Tyr702 is an important determinant of agonist binding and domain closure of the ligand-binding core of GluR2. *Mol. Pharm.* **67**:703-713.

Hermans J, Berendsen HJC, van Gunsteren WF and Postma JPM (1984) A consistent empirical potential for water-protein interactions. *Biopolymers* **23**:1513-1518.

Hess B, Bekker J, Berendsen HJC and Fraaije JGEM (1997) LINCS: A linear constraint solver

for molecular simulations. *J. Comp. Chem.* **18**:1463-1472.

Hogner A, Kastrup JS, Jin R, Liljefors T, Mayer ML, Egebjerg J, Larsen IK and Gouaux E (2002) Structural basis for AMPA receptor activation and ligand selectivity: crystal structures of five agonist complexes with the glur2 ligand-binding core. *JMB* **322**:93-109.

Holman M and Heinemann SF (1994) Cloned glutamate receptors. *Annu. Rev. Neurosci.* **17**:31-108.

Jayaraman V, Keesey R and Madden DR (2000) Ligand-protein interactions in the glutamate receptor. *Biochem.* **39**:8693-8697.

Jin R, Banke TG, Mayer ML, Traynelis SF and Gouaux E (2003) Structural basis for partial agonist action at ionotropic glutamate receptors. *Nat Neuro.* **6**:803-810.

Kabsch W and Sander C (1983) Dictionary of protein secondary structure:- pattern-recognition of hydrogen-bonded and geometrical features. *Biopolymers* **22**:2577-2637.

Kraulis PJ (1991) MOLSCRIPT: a program to produce both detailed and schematic plots of protein structures. *J. Appl. Cryst.* **24**:946-950.

Kuner T, Seeburg PH and Guy HR (2003) A common architecture for K+ channels and ionotropic glutamate receptors. *Trends Neurosci.* **26**:27-32.

Kuusinen A, Arvola M and Keinanen K (1995) Molecular dissection of the agonist binding site of an AMPA receptor. *EMBO J.* **14**:6327-6332.

Lerma J, Morales M, Vicente MA and Herreras O (1997) Glutamate receptors of the kainate type and synpatic transmission. *Trends Neurosci.* **20**:9-12.

Li G and Niu L (2004) How fast does the Glur1Qflip AMPA receptor channel open? *JBC* **279**:3990-3997.

Li G, Pei W and Niu L (2003) Channel-opening kinetics of GluR2Qflip AMPA receptor: A laser-pulse photolysis study. *Biochemistry* **42**:12358-12366.

Li H, Nowak LM, Gee KR and Hess GP (2002) Mechanism of glutamate receptor-channel function in rat hippocampal neurons investigated sing the laser-pulse photolysis (LaPP) technique. *Biochemistry* **41**:4753-4759.

Lindahl E, Hess B and D. vdS (2001) GROMACS 3.0: A package for molecular simulation and trajectory analysis. *J. Mol. Model* **7**:306-317.

Mano I, Lamed Y and Teichberg VI (1996) A Venus flytrap mechanism for activation and desensitzation of a-amino-3-hydroxy-5-methyl-4-isoxazole propionic acid receptors. *J. Biol. Chem* **271**:15299-15302.

Mano I and Teichberg VI (1998) A tetrameric subunit stoichiometry for a glutamate receptor channel complex. *Neuroreport* **9**:327-331.

Mayer ML (2005) Crystal structures of the GluR5 and GluR6 ligand binding cores: molecular mechanisms undelying kainate receptor selectivity. *Neuon* **45**:539-552.

McFeeters RL and Oswald RE (2002) Structural mobility of the extracellular ligand-binding core of an ionotropic glutamate receptor. Analysis of NMR relaxation dynamics. *Biochem.* **41**:10472-10481.

Merritt EA and Bacon J (1997) Raster3D: Photorealistic molecular graphics. *Meths. in Enzym.* **277**:505-524.

Nanao MH, Green T, Stern-Bach Y, Heinemann SF and Choe S (2005) Structure of the kainate receptor subunit GluR6 agonist-binding domain complexed with domoic acid. *Proc Natl Acad Sci USA* **102**:1708-1713.

Naur P, Vestergaard B, Skov LK, Egebjerg J, Gajhede M and Kastrup JS (2005) Crystal structure of the kainate receptor GluR5 ligand-binding core in complex with (S)-glutamate. *FEBS*

Letts. **579**:1154-1160.

Pang A, Arinaminpathy Y, Sansom MSP and Biggin PC (2003) Interdomain dynamics and ligand
binding: molecular dynamics simulations of glutamine binding protein. *FEBS Lett.*
550:168-174.

Pang A, Arinaminpathy Y, Sansom MSP and Biggin PC (2005) Comparative Molecular
Dynamics: Similar folds and similar motions? *Proteins: Struct. Funct. Bioinf.* **in press**.

Rosenmund C, Stern-Bach Y and Stevens CF (1998) The tetrameric structure of a glutamate
receptor channel. *Science* **280**:1596-1599.

Safferling M, Tichelaar W, Kummerle G, Jouppila A, Kuusinen A, Keinanen K and Madden DR
(2001) First images of a glutamate receptor ion channel: oligomeric state and molecular
dimensions of GluRB homomers. *Biochemistry* **40**:13948-13953.

Swanson GT, Kamboj SK and Cull-Candy SG (1997) Single-channel properties of recombinant
AMPA receptors depend on RNA editing, splice variation, and subunit composition. *J.
Neurosci.* **17**:58-69.

Wallace AC, Laskowski RA and Thornton JM (1995) LIGPLOT: A program to generate
schematic diagrams of protein-ligand interactions. *Prot. Eng.* **8**:127-134.

Wriggers W and Schulten K (1997) Protein domain movements: Detection of rigid domains and
visualization of hinges in comparison of atomic coordinates. *Prot. Struct. Funct. Genet.*
29:1-14.

Yamakura T and Shimoji K (1999) Subunit and site specific pharmacology of the NMDA
receptor channel. *Prog. Neurobiol.* **59**.

Footnotes

Legends for Figures

Figure 1

(A) Ribbon diagram of the crystal structure of the ligand-binding core of GluR2 in complex with glutamate. The two sub-domains are indicated as D1 and D2. Glutamate is shown in spacefill format. The chemical structures of glutamate and kainate are shown in (B) and (C) respectively. A 2-dimensional representation of the binding pocket from the LigPlot program (Wallace et al., 1995) is shown in (D). Carbon atoms are black filled circles, oxygen atoms are white filled circles, nitrogen atoms are dark-grey filled circles and water atoms are light-grey filled circles. Subsites are over-layed onto the glutamate binding position (shown also in light grey). Waters found within 4Å of bound glutamate are indicated by a W. W1 corresponds to subsite F whilst waters W2, W3 and W4 sit in close proximity to subsites C, D and E.

Figure 2

(A) Root mean square deviation (RMSD) from the initial structure (at t = 0 ns) as a function of time for all Cα atoms, shown for the Open-Apo, Closed-Apo, Glu, Kai and L650T-Kai simulations over the 20 ns duration of the simulations.

(B) Conformational stability of the D1 sub-domain. Cα RMSD of the core secondary structure elements (α-helix and β-strand regions only as defined by DSSP (Kabsch and Sander, 1983) of the D1 sub-domain fitted onto the initial co-ordinates of D1).

(C) Conformational stability of the D2 sub-domain. Cα RMSD of the core secondary structure elements (α-helix and β-strand regions only as defined by DSSP (Kabsch and Sander, 1983) of the D2 sub-domain fitted onto the initial co-ordinates of D2).

(D) Root mean square fluctuations (RMSF) of the D1 and D2 sub-domains (calculated from 2 to 20ns). All simulations followed a similar pattern but only Open-apo (black line) and Glu (grey

line) are shown for clarity. The Open-apo simulation exhibits the largest degree of fluctuation.

Secondary structure elements are indicated at the base of each plot (helices are shown as oblongs

and sheets as arrows). It can be seen that the regions of higher fluctuation correspond to the loop

regions.

Figure 3

(A) Separation between the centres-of-mass of the D1 and D2 sub-domains as a function of time

for the Open-Apo, Closed-Apo, Glu, Kai and L650T-Kai simulations.

(B) Comparison of the Open-Apo simulation with the glutamate-bound GluR2 crystal structure.

Cα RMSD of the Open-Apo simulation compared to the glutamate-bound crystal structure. The

red dashed circle indicates the time frame at which the snapshot shown in (C) was taken from.

(C) The Open-Apo structure (red) fitted to the closed (glutamate-bound) crystal structure (blue) at

t = 15.96 ns.

Figure 4

Changes in secondary structure for the (A) WT-Kai simulation and (B) the L650T-Kai

simulation. Only the change in secondary structure for a part of the D1 sub-domain, in particular

residues 421 to 481 is shown. Helices B (residues 421 to 432) and C (residues 461 to 469) are

well maintained (indicated in blue in *A* and *B*) in both simulations. (C) Schematic representation

of the WT simulation at time t = 0 ns. The two regions in sub-domain D1 observed to

preferentially form β-sheets is highlighted in blue. Residues Thr480 and Pro478 are thought to be

primarily responsible for the conformational change in this region.

Figure 5
The role of water molecules in the binding site of (A) the Glu simulation (taken at time t = 10.1

ns) and (B) the Kai simulation (at time t = 17.1 ns). Sub-sites A and B are formed by residues

from sub-domain D1 and sub-sites D, E and F are formed by residues from sub-domain D2. Sites

A, B, D, E and F in which water molecules were found over the duration of the simulations are

labelled. In the Kai simulation, the majority of protein ligand interactions are water-mediated in

stark contrast to those in the Glu simulation which are direct.

Tables

Table 1. Summary of Simulations.

Simulation	Protein	Resolution (Å)	Ligand	Time (ns)
Glu	1FTJ	1.9	Glutamate	20
Open-Apo	1FT0	2.0	-	20
Closed-Apo	1FTJ	1.9	-	20
WT-Kai	1FW0	2.0	Kainate	20
L650T-Kai	1P1N	1.6	Kainate	20

Table 2. Water Exchange Rates in the Binding Pocket. The sites are regions in close proximity to the sub-sites defined by (Armstrong and Gouaux, 2000). The values reported are the total number of times that a water in a sub-site is replaced by a different water.

Sub-site	Glutamate	Kai	Kai-L650T
A	20	253	55
B[$]	0	2	0
D	3	14	3
E	4	9	3
F	1*	13	12

*Persists for 2 ns and is subsequently not replaced.
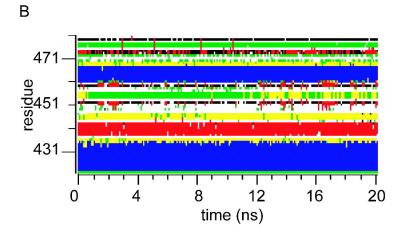
[$]No exchange as no intermediate water.

Figure 1

A

B

C

glutamate

kainate

D

Figure 2

A

B

C

D

Figure 3

A

B

C

Figure 4

Figure 5

A t = 4.755 ns

Arg485   Pro478

Glu705

Thr655

B t = 4.830 ns

Arg485   Pro478

Glu705

Thr655

C t = 5.0 ns

Arg485   Pro478

Glu705

Thr655

D t = 5.025 ns

A

t = 0 ps

Pro478

Arg485

Glu705

Thr650

B

t = 35 ps

Pro478

Arg485

Glu705

Thr650

C

t = 60 ps

Pro478

Arg485

Glu705

Thr650

D

t = 125 ps

Pro478

Arg485

Glu705

Thr650